

## Metastable One-Dimensional $\text{AgCl}_{1-x}\text{I}_x$ Solid-Solution Wurzite “Tunnel” Crystals Formed within Single-Walled Carbon Nanotubes

Jeremy Sloan,<sup>\*,†,§</sup> Mauricio Terrones,<sup>¶,‡</sup> Stefan Nufer,<sup>¶</sup> Steffi Friedrichs,<sup>†</sup> Sam R. Bailey,<sup>†</sup> Hee-Gweon Woo,<sup>||</sup> Manfred Rühle,<sup>¶</sup> John L. Hutchison,<sup>§</sup> and Malcolm L. H. Green<sup>†</sup>

*Inorganic Chemistry Laboratory, South Parks Road, Oxford, OX1 3QR, United Kingdom, Department of Materials, South Parks Road, Oxford, OX1 3PH, United Kingdom, Max Planck Institut für Metallforschung, Seestrasse 92, D-70174 Stuttgart, Germany, and Department of Chemistry, Chonnam National University, 300 Yongbong-dong, Puk-ku, Kwangju, 500-757, Korea*

Received October 18, 2001

Single-walled carbon nanotubes (SWNTs)<sup>1</sup> are 1–2 nm diameter  $\text{sp}^2$  carbon cylinders capable of hosting a variety of species, including 1D crystals of metals,<sup>2</sup> metal salts<sup>2</sup> and oxides;<sup>3</sup> helical iodine chains;<sup>4</sup> and chains of fullerene<sup>5a</sup> or endofullerene molecules.<sup>5bc</sup> The synthesis of such composites has been driven by a desire to study such materials when confined to a low-dimensional environment. For example, it has been possible to image individual fullerenes<sup>5</sup> and bulk crystalline structures confined to the molecular scale.<sup>2–4</sup> Using high-resolution transmission electron microscopy (HRTEM) image restoration, it has been possible to study the latter on an atom-by-atom basis<sup>2f</sup> and also to determine simultaneously the chirality of the host SWNTs.<sup>3b</sup> Despite this level of characterization, it has proved difficult to study inclusions containing more than two elements. While we previously inserted  $\text{AgBr}$ – $\text{AgCl}$  and  $\text{KCl}$ – $\text{UCl}_4$  mixtures into SWNTs,<sup>2b</sup> detailed information concerning local crystallinity or composition was unavailable. Here we describe the application of HRTEM and spatially resolved electron energy loss spectroscopy (EELS) to the systematic characterization of a eutectic  $\text{AgCl}$ – $\text{AgI}$  mixture formed inside SWNTs. This composition contains one strongly scattering halogen (i.e.: I,  $Z = 53$  vs Cl,  $Z = 17$ ), which should facilitate preferential imaging via HRTEM and scanning transmission electron microscopy (STEM). We also show how the eutectic forms metastable 1D “tunnel” structures within SWNTs.

Samples of SWNTs were prepared by catalytic arc synthesis<sup>6</sup> and a premelted molten 53:47 mol % mixture conforming to the  $\text{AgCl}$ – $\text{AgI}$  eutectic<sup>7</sup> was introduced via a published method.<sup>2b</sup> The specimen was examined in a 300 kV JEOL 3000F HRTEM (0.16 nm point resolution). Energy-dispersive X-ray spectra (EDX) were obtained with a 0.5 nm probe (LINK “ISIS” system). EELS line scans were obtained with an energy dispersion of 0.1 eV/channel and a 1.0 nA/1.0 nm<sup>2</sup> probe in a VG HB501UX STEM with a Gatan Digi-PEELS 766 detector. Pre- and post-scan high-angle annular dark field (HAADF) images were obtained from the specimen.

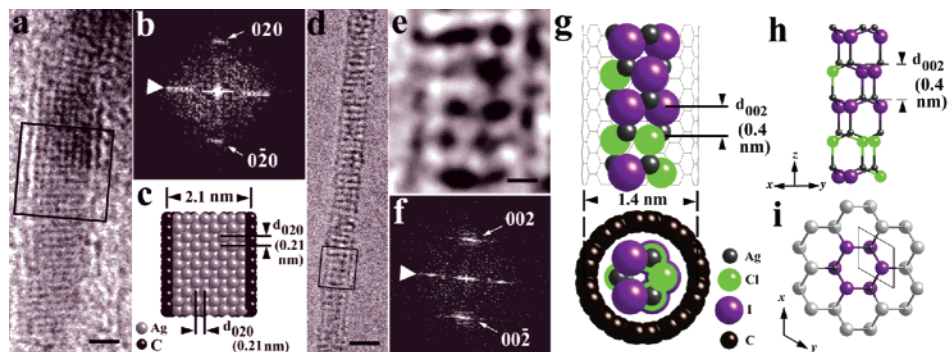
HRTEM showed that ca. 50% of the observed SWNTs contained filling that was predominantly crystalline, although ca. 30% was glassy. The crystalline filling consisted of the following: (i) metallic Ag filling (Figure 1a–c), presumed to originate from dissociation of the halide mixture (cf. ref 2b), and (ii) crystalline halide filling (Figure 1d–i). The latter is assumed to be metastable as solid eutectic  $\text{AgCl}$ – $\text{AgI}$  should be polycrystalline. EDX spectra obtained from (ii) indicated that it contained Ag, Cl, and I.

Figure 1a shows a ca. 2 nm diameter SWNT filled with a *fcc* type Ag metal for which  $\langle 010 \rangle$  is parallel to the SWNT growth axis and  $\langle 001 \rangle$  is parallel to the electron beam. Measurements from the image and corresponding fast Fourier transform (Figure 1b) produced an average lattice spacing orthogonal to the SWNT axis of ca. 0.21 nm, corresponding to  $d_{020}$  for bulk Ag.<sup>8</sup> The SWNT walls are visible as dark lines either side of the Ag nanocrystal, which is visualized as eight  $\{200\}$  layers arranged parallel to the SWNT axis (Figure 1c).

Figure 1d–f shows a HRTEM image, enlargement, and corresponding FFT of crystalline halide filling formed in a 1.4 nm diameter SWNT. An average periodicity of ca. 0.4 nm was established along the SWNT axis, which was characteristic of all the crystalline halide filling. Figure 1e reveals that the microstructure consists of an ordered array of distorted dark spots. The 0.4 nm spacing and spot configuration suggest a 1D “tunnel” structure derived from wurzite  $\text{AgI}$ <sup>9</sup> (i.e. Figure 1g–i). Wurzite  $\text{AgI}$  consists of stacked hexagonal double layers of Ag and I separated by  $\sim 0.37$  nm (i.e.  $d_{002}$ <sup>9</sup>). According to our model, each dark spot corresponds to a staggered X–Ag–X or Ag–X–Ag column (Figure 1g, bottom). Inspection of Figure 1e reveals that the dark spots vary unsystematically in contrast, an effect that we attribute to random distribution of weaker scattering Cl and stronger scattering I over the X sites (Figure 1g,h; see also Supporting Information). It is noteworthy that the formation of such a structure would result in reduction in coordination for Ag from tetrahedral to trigonal, which may explain the small increase in  $d_{002}$  (cf. 4:4 KI in SWNTs<sup>2e</sup>).

EELS line scans were used to probe the local compositions of SWNT bundles such as the example given by the HAADF image in Figure 2a. Figure 2b shows an end-on view of a 3D plot of 26 spectra obtained along I–II. The height of the dominant C–K absorption edge gives an indication of the thickness of the bundle with respect to probe position. A representative EELS spectrum with resolved Cl–L<sub>2,3</sub>, Ag–M<sub>4,5</sub>, and I–M<sub>4,5</sub> edges is shown in Figure 2c. The I and Cl edges were always observed together whenever halide was detected, indicating that the  $\text{AgCl}$ – $\text{AgI}$  mixture melted congruently into the SWNTs. The perspective view of the 3D plot (Figure 2d) shows the evolution of the EELS spectra along I–II. The Cl, Ag, and I edges are absent from the group of peaks corresponding to the SWNT nearest to I, indicating that this tube is empty according to the configuration inset in Figure 2d. Cl:I ratios determined from counts obtained from integrated Cl and I absorption edges varied from ca. 10:1 to 1:10, thus supporting the observation above that local concentrations of Cl and I vary on an unsystematic basis. Additional EELS line scans confirmed the

<sup>†</sup> Inorganic Chemistry Laboratory.  
<sup>§</sup> Department of Materials.  
<sup>¶</sup> Max Planck Institute.  
<sup>‡</sup> Present address: IPICYT, México.  
<sup>||</sup> Chonnam National University.



**Figure 1.** (a) HRTEM image of Ag crystal within a SWNT (scale bar = 1 nm). (b) FFT from the boxed region in part a. Arrow indicates scattering from SWNT. (c) Structure model. (d) HRTEM image of crystalline  $\text{AgCl}_{1-x}\text{I}_x$  filling (scale bar = 2 nm). (e) Detail from part d (scale bar = 0.2 nm). (f) FFT from part d. (g) Side-on and end-on representations of proposed “tunnel” structure. (h) Staggered ball-and-stick model showing Ag coordination. (i) Derivation of tunnel structure from the AgI wurzite structure.

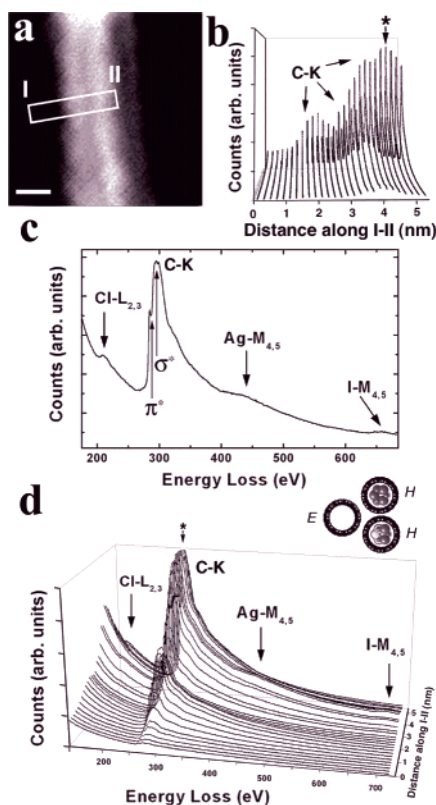


**Figure 2.** (a) HAADF image (scale bar = 2 nm). (b) End-on view of the 3D plot of EELS spectra obtained along I–II. (c) EELS spectrum indicated in parts b and d. (d) 3D EELS plot and predicted filling configuration (key: E = empty SWNT; H = halide filled SWNT).

formation of elemental Ag in some SWNTs (see Supporting Information).

Our results show that a metastable  $\text{AgCl}_{1-x}\text{I}_x$  solid solution has been formed within SWNT capillaries thus providing the first evidence for the formation of a ternary crystalline phase inside SWNTs. The  $\text{AgCl}_{1-x}\text{I}_x$  solid solution formed a tunnel structure derived from wurzite AgI with Cl and I distributed randomly over the halogen sites. Spatially resolved EELS revealed local variations in Cl:I ratios and formation of metallic Ag in some SWNTs. The

1D  $\text{AgCl}_{1-x}\text{I}_x$  crystals represent the lowest dimensionality recorded for any solid-solution crystal system.

**Acknowledgment.** We acknowledge the Petroleum Research Fund, administered by the ACS (Grant No. 33765-AC5), and the EPSRC (Grant Nos. GR/L59238 and GR/L22324). J.S. is indebted to the Royal Society, M.T. to the A. v. Humboldt Stiftung, S.N. to the Deutsche Forschungsgemeinschaft (Grant No. Ru 342/11-2), S.F. to BMBF and Fonds der Chemischen Industrie, and H.G.W. to the RSC Journals Grants 2000 and KRF grant (2000-D00165).

**Supporting Information Available:**  $\text{AgCl}$ – $\text{AgI}$  phase diagram; derivation of the 1D wurzite tunnel structure and HRTEM image simulation; additional integrated EELS profiles (PDF). This material is available free of charge via the Internet at <http://pubs.acs.org>.

## References

- (1) (a) Iijima, S.; Ichihashi, T. *Nature* **1993**, *363*, 603–605. (b) Bethune, D. S.; Kiang, C. H.; de Vries, M. S.; Gorman, G.; Savoy, R.; Vazquez, J.; Beyers, R. *Nature* **1993**, *363*, 605–607.
- (2) (a) Sloan, J.; Hammer, J.; Zweifka-Sibley, M.; Green, M. L. H. *J. Chem. Soc., Chem. Commun.* **1998**, 347–348. (b) Sloan, J.; Wright, D. M.; Woo, H.-G.; Bailey, S.; Brown, G. York, A. P. E.; Coleman, K. S.; Hutchison, J. L.; Green, M. L. H. *J. Chem. Soc., Chem. Commun.* **1999**, 699–700. (c) Kiang, C. H.; Choi, J. S.; Tran, T. T.; Bacher, A. D. *J. Phys. Chem. B* **1999**, *103*, 7449–7451. (d) Govindaraj, A.; Satiskumar, B. C.; Nath, M.; Rao, C. N. R. *Chem. Mater.* **2000**, *12*, 202–205. (e) Sloan, J.; Novotny, M. C.; Bailey, S. R.; Brown, G.; Xu, C.; Williams, V. C.; Friedrichs, S.; Flahaut, E.; Callendar, R. L.; York, A. P. E.; Coleman, K. S.; Green, M. L. H.; Dunin-Borkowski, R. E.; Hutchison, J. L. *Chem. Phys. Lett.* **2000**, *329*, 61–65. (f) Meyer, R. R.; Sloan, J.; Dunin-Borkowski, R. E.; Kirkland, A. I.; Novotny, M. C.; Bailey, S. R.; Hutchison, J. L.; Green, M. L. H. *Science* **2000**, *289*, 1324–1326.
- (3) (a) Mittal, J.; Monthieux, M.; Allouche, H.; Stephan, O. *Chem. Phys. Lett.* **2001**, *339*, 311–318. (b) Friedrichs, S.; Sloan, J.; Green, M. L. H.; Hutchison, J. L.; Meyer, R. R.; Kirkland, A. I. *Phys. Rev. B* **2001**, *64*, 045406/1–045406/8.
- (4) Fan, X.; Dickey, E. C.; Eklund, P. C.; Williams, K. A.; Grigorian, L.; Buczko, R.; Pantelides, S. T.; Pennycook, S. J. *Phys. Rev. Lett.* **2000**, *84*, 4621–4624.
- (5) (a) Smith, B. W.; Monthieux, M.; Luzzi, D. E. *Nature* **1998**, *396*, 323–324. (b) Smith, B. W.; Luzzi, D. E.; Achiba, Y. *Chem. Phys. Lett.* **2000**, *331*, 137–142. (c) Suenaga, K.; Tence, M.; Mory, C.; Colliex, C.; Kato, H.; Okazaki, T.; Shinohara, H.; Hirahara, K.; Bandow, S.; Iijima, S. *Science* **2000**, *290*, 2280–2281.
- (6) Journet, C.; Maser, W. K.; Bernier, P.; Loiseau, A.; Lamy de la Chapelle, M.; Lefrant, S.; Deriard, P.; Fisher, J. E. *Nature* **1997**, *388*, 756–758.
- (7) Reproduced in the Supporting Information from: Cornell, K.; Dyson, R. W. *Brit. J. Appl. Phys. (J. Phys. D)* **1969**, *2*, 305–307.
- (8) Liu, L. G.; Bassett, W. A. *J. Appl. Phys.* **1973**, *44*, 1475–1479.
- (9) Yoshiasa, A.; Koto, K.; Kanamura, F.; Emura, S.; Horiuchi, H. *Acta Crystallogr. B* **1987**, *43*, 434–440.

JA0173270